

Transgenic cyclooxygenase-2 overexpression sensitizes mouse skin for carcinogenesis

Karin Müller-Decker, Gitta Neufang, Irina Berger, Melanie Neumann, Friedrich Marks, and Gerhard Fürstenberger

PNAS 2002;99:12483-12488; originally published online Sep 9, 2002;
doi:10.1073/pnas.192323799

This information is current as of March 2007.

Online Information & Services	High-resolution figures, a citation map, links to PubMed and Google Scholar, etc., can be found at: www.pnas.org/cgi/content/full/99/19/12483
References	This article cites 30 articles, 11 of which you can access for free at: www.pnas.org/cgi/content/full/99/19/12483#BIBL This article has been cited by other articles: www.pnas.org/cgi/content/full/99/19/12483#otherarticles
E-mail Alerts	Receive free email alerts when new articles cite this article - sign up in the box at the top right corner of the article or click here .
Rights & Permissions	To reproduce this article in part (figures, tables) or in entirety, see: www.pnas.org/misc/rightperm.shtml
Reprints	To order reprints, see: www.pnas.org/misc/reprints.shtml

Notes:

Transgenic cyclooxygenase-2 overexpression sensitizes mouse skin for carcinogenesis

Karin Müller-Decker^{*†}, Gitta Neufang^{*}, Irina Berger[‡], Melanie Neumann^{*}, Friedrich Marks^{*}, and Gerhard Fürstenberger^{*}

^{*}Research Program Tumor Cell Regulation, Deutsches Krebsforschungszentrum, and [‡]Department of Pathology, Ruprecht-Karls-University, 69120 Heidelberg, Germany

Edited by Philip Needleman, Pharmacia Corporation, St. Louis, MO, and approved July 29, 2002 (received for review May 30, 2002)

Genetic and pharmacological evidence suggests that overexpression of cyclooxygenase-2 (COX-2) is critical for epithelial carcinogenesis and provides a major target for cancer chemoprevention by nonsteroidal antiinflammatory drugs. Transgenic mouse lines with keratin 5 promoter-driven COX-2 overexpression in basal epidermal cells exhibit a preneoplastic skin phenotype. As shown here, this phenotype depends on the level of COX-2 expression and COX-2-mediated prostaglandin accumulation. The transgenics did not develop skin tumors spontaneously but did so after a single application of an initiating dose of the carcinogen 7,12-dimethylbenz[*a*]anthracene (DMBA). Long-term treatment with the tumor promoter phorbol 12-myristate 13-acetate, as required for tumorigenesis in wild-type mice, was not necessary for transgenics. The ratios of squamous cell carcinomas to papillomas and of sebaceous gland adenomas to papillomas plus squamous cell carcinomas were increased markedly in transgenic mice treated with DMBA alone compared with DMBA/phorbol 12-myristate 13-acetate-treated transgenic and wild-type mice. Thus, COX-2 overexpression, which leads to high levels of epidermal prostaglandin E₂, prostaglandin F_{2α}, and 15-deoxy^{Δ12,14}-PGJ₂, is insufficient for tumor induction but transforms epidermis into an "autopromoted" state, i.e., dramatically sensitizes the tissue for genotoxic carcinogens.

Nonsteroidal antiinflammatory drugs (NSAIDs) prevent prostaglandin (PG) biosynthesis through inhibition of cyclooxygenase (COX) activity and are used as antiinflammatory, analgesic, and fever-relieving drugs (1). Moreover, in animal studies NSAIDs interrupted the development of various epithelial tumors, and in man long-term intake of these drugs substantially reduced the risk for developing colorectal cancer (2). The COX-2 isozyme has been identified as a major target for the antitumor activities of NSAIDs (3).

In contrast to the constitutively and ubiquitously expressed COX-1, COX-2 is not expressed in most tissues but becomes transiently induced in response to growth factors, proinflammatory cytokines, mechanical tissue damage, and UV light (1, 3). However, COX-2 is constitutively overexpressed in various preneoplasias and epithelial tumors, suggesting that this isoform plays a role in cancer development (2–4). Furthermore, newly developed COX-2-selective inhibitors strongly suppressed the development of epithelial cancers in animals (5–7) and significantly reduced the number of colorectal polyps in patients suffering from familial adenomatous polyposis coli (8).

Although COX-1 expression does not change in the course of tumor development, aberrant expression of COX-2 is also a consistent feature of nonmelanoma skin cancer in man and mice. COX-2 was found to be overexpressed in premalignant actinic keratoses and papillomas as well as squamous cell carcinomas. This overexpression was observed in the tumor parenchyme (basal keratinocytes) of papillomas and throughout the epithelium of actinic keratoses and cells of the tumor stroma (6, 9–11). COX-2-selective inhibitors exhibited chemopreventive activity against chemically (6) and UV light-induced (11, 12) skin carcinogenesis in mice. Data from gene knockout (13, 14) and transgenic mice (15, 16) provide support for the hypothesis that

there is a causal relationship between COX-2 overexpression and tumor development. Recently, we have shown that the keratin 5 (K5) promoter-driven overexpression of COX-2 in basal cells of interfollicular epidermis and the pilosebaceous unit led to a preneoplastic skin phenotype in 4 of 4 high-expression mouse lines (15).

To delineate COX-2 functions for carcinogenesis, we have used the initiation–promotion model (2) for the induction of skin tumors in wild-type (wt) NMRI mice and COX-2 transgenic mouse lines. This multistage model allows the analysis of the carcinogenic process in terms of distinct stages, i.e., initiation by application of a subcarcinogenic dose of a carcinogen such as 7,12-dimethylbenz[*a*]anthracene (DMBA), promotion by repeated applications of a tumor promoter such as phorbol 12-myristate 13-acetate (PMA), and malignant progression, which may occur spontaneously or after administration of additional carcinogen (2). As shown here, overexpression of COX-2 targeted to basal keratinocytes contributes to skin-tumor promotion and progression by establishing an autopromoted skin phenotype, i.e., the initiating dose of DMBA is sufficient to induce skin carcinogenesis in COX-2 transgenic mice.

Materials and Methods

Materials. ELISA-BSA, DMBA, and PMA were purchased from Sigma. Affinity-purified polyclonal rabbit anti-mouse keratin 10 (K10) was from Babco (Richmond, CA); purified monoclonal rat anti-mouse CD31 was from Becton Dickinson; rabbit anti-mouse Ki67, alkaline phosphatase-conjugated goat anti-rabbit IgG, and Cy3-donkey anti-rat IgG were from Dianova (Hamburg, Germany); polyclonal goat anti-human COX-2 (SC1745) and peroxidase-conjugated goat anti-rabbit IgG were from Santa Cruz Biotechnology; and Alexa fluor 488-labeled donkey anti-goat IgG was from Molecular Probes. PGE₂, PGF_{2α}, and 6-keto-PGF_{1α} enzyme immunoassay kits were from Cayman Chemical (Ann Arbor, MI), and the 15-deoxy^{Δ12,14}-PGJ₂ kit was from Assay Designs (Ann Arbor, MI). Rodent diet 5010 and rodent diets 5010 supplemented with 1,500 ppm celecoxib or 500 ppm valdecoxib, i.e., equipotent COX-2-selective inhibitory doses (17, 18), were kindly provided by K. Seibert (Amersham Pharmacia).

Animals. wt NMRI mice (outbred strain from RCC, Füllinsdorf, Switzerland) and K5.COX-2 transgenic lines 19^{+/-} and 667^{+/-}, generated as described (15), were kept in the Deutsches Krebsforschungszentrum under an artificial day/night rhythm and fed Altromin standard food pellets and water *ad libitum* if not stated otherwise. All animal experiments have been ap-

This paper was submitted directly (Track II) to the PNAS office.

Abbreviations: PG, prostaglandin; COX, cyclooxygenase; K5, keratin 5; K10, keratin 10; wt, wild type; DMBA, 7,12-dimethylbenz[*a*]anthracene; PMA, phorbol 12-myristate 13-acetate.

[†]To whom reprint requests should be addressed at: Deutsches Krebsforschungszentrum, INF 280, 69120 Heidelberg, Germany. E-mail: K.Mueller-Decker@DKFZ-Heidelberg.de.

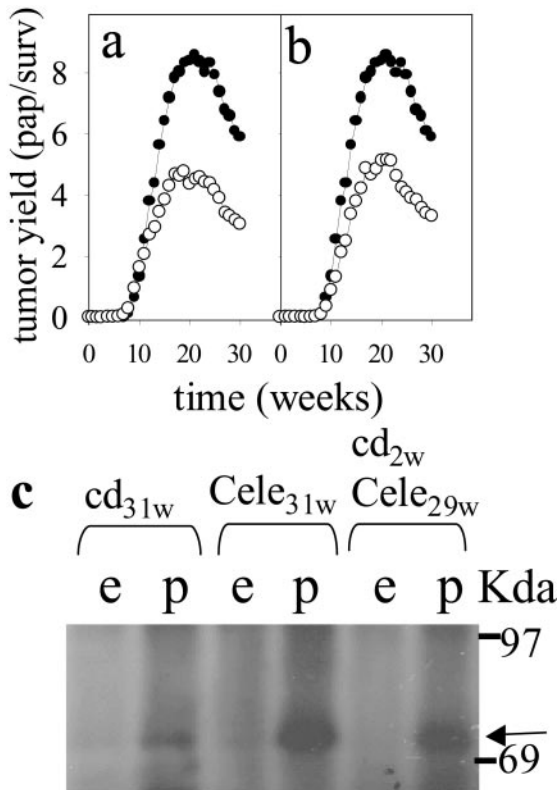


Fig. 1. Inhibition of tumor promotion by COX-2 inhibition. By using the multistage mouse skin-carcinogenesis model, NMRI mice were initiated with a single DMBA treatment at time 0. Two weeks later, promotion with PMA treatment was started and continued until week 30. (a and b) Tumor yield in number of papillomas/survivors (pap/surv) is plotted vs. time after initiation for animals fed a celecoxib-containing diet starting 1 week before DMBA initiation (a, ○) or starting 1 week before PMA promotion (b, ○) compared with animals receiving a drug-free control diet (a and b, ●). (c) COX-2 expression was detected by immunoblot analysis in papillomas (p) but not in surrounding epidermis (e) collected from animals fed with a drug-free control diet (cd, 31 weeks) or a celecoxib-containing diet beginning 1 week before DMBA initiation and continuing for the duration of the experiment (cele, 31 weeks) or 1 week before PMA promotion (cele, 29 weeks). Arrow, COX-2 signal.

proved by the Governmental Committee for animal experimentation (License 002/98).

Treatments. For epicutaneous applications the dorsal skin was shaved with electric clippers 3 or 7 days before treatment. To study the effect of a COX-2-selective inhibitor on the transgene-induced phenotype, rodent diet 5010 containing 500 ppm valdecoxib was fed to transgenic mice starting on day one after birth for 3 months by delivering the diet to nursing mice for 4 weeks and later as regular chow. Biopsies were frozen immediately at $\leq -70^{\circ}\text{C}$ or processed for immunohistochemistry. For initiation-promotion experiments, groups of 10–74 7-week-old female NMRI mice or transgenic lines were initiated by a single epicutaneous application of either 0.1 ml acetone or 0.1 μmol DMBA in 0.1 ml acetone. Beginning 2 weeks later, the mice were treated each twice weekly with 0.1 ml acetone or 5 nmol PMA in 0.1 ml of acetone for 28 weeks. Papilloma and carcinoma development was monitored up to week 50 without further treatment. The tumor incidence (tumor bearers/survivors in percent) and yield (number of tumors/survivors) were recorded weekly. Tumors were identified first macroscopically and later by histological diagnosis. For the experiments with the COX-2-selective inhibitor celecoxib (1,500 ppm), the rodent diet 5010

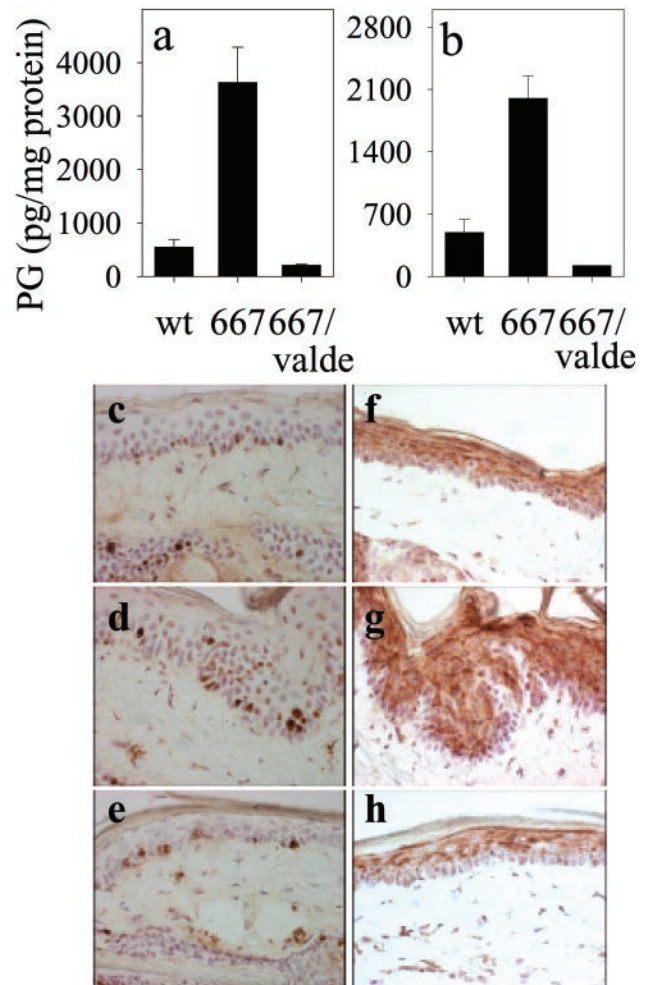


Fig. 2. Suppression of the COX-2 transgene-induced PG levels and phenotype by COX-2 inhibition. The levels (mean \pm SEM) of PGE_2 (a) and $\text{PGF}_{2\alpha}$ (b) were determined for tail skin of wt NMRI ($n = 7$), K5.COX-2/667 $^{+/+}$ transgenic mice fed with a control diet (667, $n = 8$), and K5.COX-2/667 $^{+/+}$ transgenic mice receiving a valdecoxib-containing (valde) diet (667/valdecoxib, $n = 3$); P values for PGE_2 and $\text{PGF}_{2\alpha}$ were ≤ 0.0001 . The histology and localization of Ki67-positive keratinocytes in the interfollicular epidermis of tail-skin sections are shown for wt (c), K5.COX-2/667 $^{+/+}$ transgenic (d), and valdecoxib-treated K5.COX-2/667 $^{+/+}$ transgenic mice (e). K10 staining in tail-skin sections is shown for wt (f), K5.COX-2/667 $^{+/+}$ transgenic (g), and valdecoxib-treated K5.COX-2/667 $^{+/+}$ transgenic mice (h). [Magnification, $\times 400$ (c–h).]

was replaced by celecoxib-containing diet starting either 1 week before or 1 week after initiation and continued for the duration of the experiment.

Immunoblot Analysis. Immunoprecipitation of COX-2 and COX-1 as well as immunoblot analysis were carried out by using isoenzyme-specific antisera as described (6, 10).

Histochemistry and Immunohistochemistry. For hematoxylin/eosin staining, skin was fixed in PBS-buffered 4% paraformaldehyde for 16 h before embedding into paraffin. COX-2, Ki67, K10, and CD31 stainings were performed with 5- μm cryosections according to a protocol described (6) except that 1% ELISA-BSA in PBS was used as blocking solution and sections were fixed in acetone for 10 min. Primary antibodies were diluted 1:50 and peroxidase- or fluorochrome-conjugated secondary antibodies 1:100 in blocking solution. For double-immunofluorescence analysis, primary antibodies were diluted 1:50 and secondary

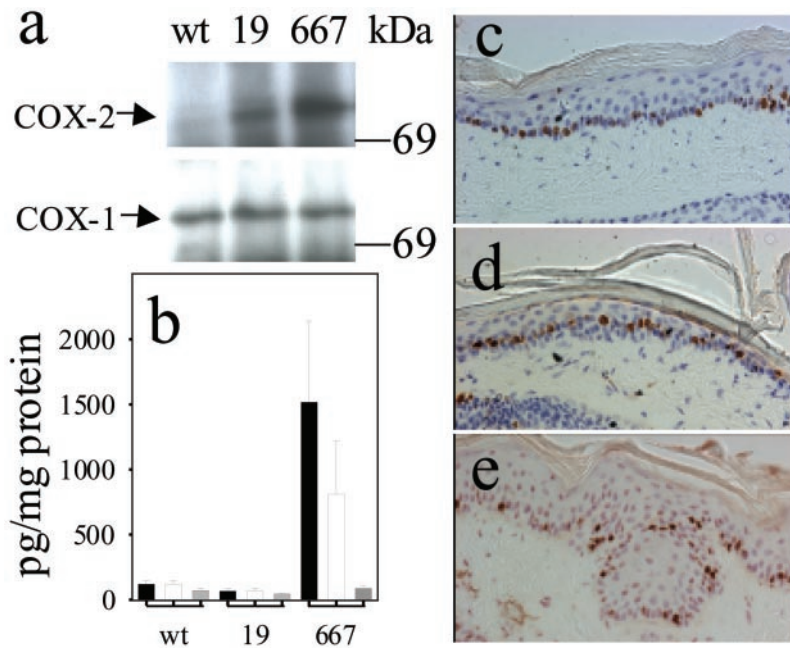


Fig. 3. COX isozyme expression, PG levels, and skin morphology in age-matched transgenic as compared with wt mice. (a) COX isozyme expression in epidermis from wt mice and the transgenic lines K5.COX-2/19^{+/-} (19) and K5.COX-2/667^{+/-} (667). (b) Epidermal PG levels (mean ± SEM; PGE₂, black bars; PGF_{2α}, white bars; 6-keto-PGF_{1α}, gray bars) in wt mice (*n* = 5) and the transgenic mice K5.COX-2/19^{+/-} (19, *n* = 5) and K5.COX-2/667^{+/-} (667, *n* = 3); *P* values for PGE₂ and PGF_{2α} (wt vs. K5.COX-2/667^{+/-}) were ≤ 0.036 . Epidermal histology and localization of Ki67-positive keratinocytes are shown for skin sections from wt mice (c) and the transgenic mice of K5.COX-2/19^{+/-} (d) and K5.COX-2/667^{+/-} (e). [Magnification: $\times 400$.]

antibodies 1:200 in blocking solution. Specimens were mounted with Eukitt or DAKO fluorescence mounting medium (DAKO) and examined by an Axioskop 2 microscope connected to an AxioCam camera using AXIOVISION 2.05 software (Zeiss).

Determination of PG Concentrations in Epidermis and Skin. Immediately after excision, skin was frozen at 0°C. Epidermis was scraped off with a scalpel at -70°C and stored in liquid nitrogen. Individual epidermal or skin samples were homogenized in a Teflon mortar precooled in liquid nitrogen by using a micro dismembrator S (Braun, Melsungen, Germany, 2,500 rpm/30 sec). Tissue powder was suspended in 2 ml of ice-cold ethanol containing 10 nCi (1 Ci = 37 GBq) of [³H]PGE₂ as an internal standard. After thorough mixing for 30 sec and centrifugation (10 min, 3,000 \times g, 4°C), the supernatant was collected and diluted to 15% ethanol with 0.1 M sodium formate buffer, pH 3.1. PGs were enriched by solid-phase extraction on 500 mg of C18 (EC) isolate silica cartridges that were rinsed with 5 ml each of 15% ethanol/aqua bidest (vol/vol), aqua bidest, and *n*-hexane. PGs were eluted with 4 ml of ethyl acetate. The dried lipids were resuspended in 1 ml of enzyme immunoassay buffer delivered within the enzyme immunoassay kits that were used according to supplier instructions. The protein pellets were dissolved in 8 M urea and used for measurement of protein concentrations by means of the Bio-Rad protein-detection kit. Concentrations (pg/mg of protein) represent mean ± SEM for *n* = 3–8 samples. The Wilcoxon rank-sum test was used for one-way comparisons.

Results

Suppression of Skin-Tumor Promotion but Not Initiation by a COX-2-Selective Inhibitor. We tested the activity of the COX-2-selective inhibitor celecoxib (17) on chemically induced tumor formation in the skin of NMRI mice. Mice fed with a celecoxib-containing diet throughout the promotion phase of the experiment developed $\approx 50\%$ less papillomas compared with controls (Fig. 1a).

Feeding of the drug-containing diet before and during the initiation phase (Fig. 1 *a* vs. *b*) had no additional suppressive effect on tumor yield, suggesting that COX-2 activity is involved in tumor promotion but not initiation. COX-2 was expressed only in papillomas and not in the surrounding tumor-free epidermis (Fig. 1c). COX-2-expression levels were increased slightly in the papillomas of celecoxib-treated mice compared with the levels in tumors of control mice. COX-1 levels were similar in normal and neoplastic epidermis for all treatment groups.

Development of the Epidermal Phenotype of K5.COX-2 Transgenic Mice Depends on the Level of COX-2 Expression and COX-2-Mediated PG Synthesis. We previously reported that K5 promoter-driven COX-2 overexpression in basal cells of interfollicular and follicular epidermis exhibited a preneoplastic skin phenotype in 4 of 4 high-expression transgenic mouse lines (15). When transgenic mice of the high-expression line K5.COX-2/667^{+/-} were fed the COX-2-selective inhibitor valdecoxib (18) for 3 months postnatally, PGE₂ and PGF_{2α} accumulation in skin was reduced to wt levels, whereas transgenic littermates fed with a drug-free control diet had highly elevated PG levels (Fig. 2 *a* and *b*). Moreover, the usual phenotype for the interfollicular tail epidermis of these transgenic mice, i.e., basal cell hyperplasia with focal endophytic growth of the hyperplastic epithelium (Fig. 2 *d* and *g*), did not develop during valdecoxib treatment (Fig. 2 *e* and *h*). Instead, epidermal morphology resembled that of wt with a uniform thickness consisting of one layer of basal keratinocytes and 3–5 suprabasal cell layers (Fig. 2 *c* and *f*). In addition, expression of the proliferation marker Ki67 was restricted to the basal keratinocytes of wt NMRI mice (Fig. 2c) and valdecoxib-fed transgenics (Fig. 2e), whereas in untreated transgenics Ki67-positive keratinocytes were observed regularly in suprabasal cells (Fig. 2d). For the transgenics, treatment with valdecoxib resulted in retention of the expression pattern of differentiation-associated K10 in the epidermis (Fig. 2h), i.e., a

Table 1. Tumor induction with the initiation–promotion protocol in COX-2-transgenic mouse lines

Line	Tumor induction			
	Incidence		Yield	
	18 weeks	24 weeks	18 weeks	24 weeks
wt	80	95	4.2	5.2
19 ^{+/-}	85	100	3.7	5.7
667 ^{+/-}	65	77	2.6	3.8

Groups of 20 mice were initiated by DMBA and promoted 2 weeks later by twice-weekly applications of PMA continued for 30 weeks. Tumor incidence (number of tumor bearers/survivors in %) and tumor yield (number of tumors/survivors) were recorded after 18 and 24 weeks of promotion. Histological diagnosis revealed that 77% of tumors were papillomas, and 20% were sebaceous gland adenomas, and 3% were squamous cell carcinomas independent of the treatment group.

uniform distribution throughout the suprabasal compartment as in wt epidermis (Fig. 2*f*). K10-negative suprabasal keratinocytes were observed only in the epidermis of untreated transgenics (Fig. 2*g*). The results presented above indicate that valdecoxib-dependent suppression of COX-2 activity inhibited the development of the transgenic phenotype.

The degree of development of the transgenic phenotype depended critically on both the expression level of the COX-2

transgene and the level of COX-2-mediated PG synthesis. COX-2 protein was only weakly expressed in the transgenic mouse line K5.COX-2/19^{+/-} compared with the strong expression in the epidermis of the K5.COX-2/667^{+/-} line mentioned above, whereas COX-1-expression levels were comparable for the two genotypes (Fig. 3*a*). Epidermal levels of PGE₂ and PGF_{2α} were similarly low in wt and K5.COX-2/19^{+/-} mice compared with the strongly increased levels in K5.COX-2/667^{+/-} mice. In contrast, epidermal levels of 6-keto-PGF_{1α} did not depend on transgene expression (Fig. 3*b*). With respect to morphology and localization of Ki67-positive keratinocytes, the epidermis of K5.COX-2/19^{+/-} mice resembled that of wt rather than K5.COX-2/667^{+/-} mice (Fig. 3 *c–e*).

The Effect of the K5.COX-2 Transgene on Tumor Development. When epidermal tumors were induced according to the initiation–promotion protocol, tumor incidence and yield were similar for wt and low-expression K5.COX-2/19^{+/-} mice but somewhat reduced for high-expression K5.COX-2/667^{+/-} mice (Table 1). As expected, a single application of a subcarcinogenic (initiating) dose of DMBA alone did not lead to skin-tumor development in wt animals. In contrast, K5.COX-2/667^{+/-} transgenic mice exhibited a strong tumor response after initiation only (Fig. 4 *a* and *b*), whereas the low-expression K5.COX-2/19^{+/-} mice did not develop tumors without promotion. Thus, tumor development depended on the expression level of the transgene, which

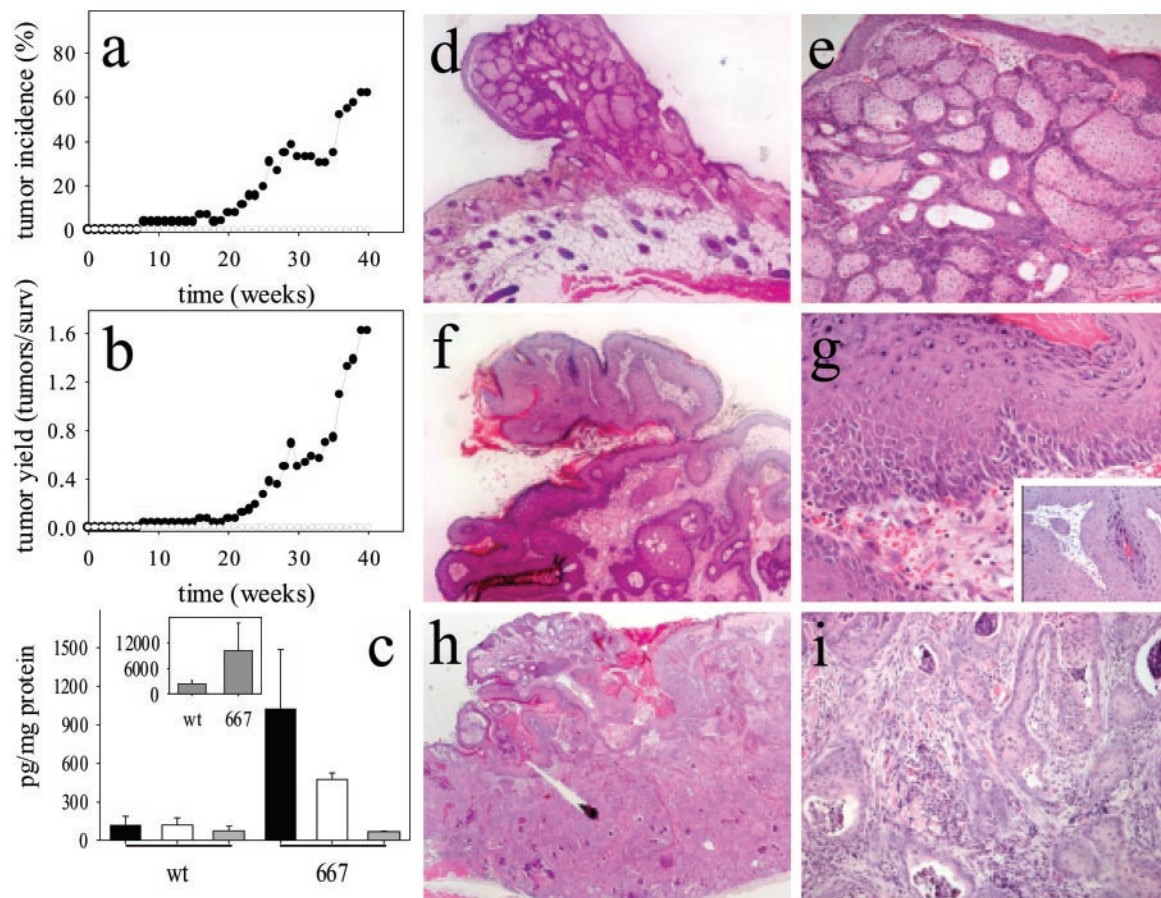


Fig. 4. Tumor formation in skin of K5.COX-2/667^{+/-} transgenic mice after DMBA initiation alone. Tumor incidence (*a*) and yield (*b*) after DMBA initiation alone of wt (○) and K5.COX-2/667^{+/-} transgenic mice (●). Epidermal PG levels (*c*, mean ± SEM; PGE₂, black bars; PGF_{2α}, white bars; 6-keto-PGF_{1α}, gray bars; 15-deoxy-Δ^{12,14}-PGJ₂, *Inset*) are shown for tumor-bearing K5.COX-2/667^{+/-} transgenic (667, *n* = 3) and age-matched tumor-free wt (*n* = 5) mice; *P* values for PGE₂, PGF_{2α}, and 15-deoxy-Δ^{12,14}-PGJ₂ were 0.036. Representative hematoxylin/eosin-stained sections are shown for sebaceous gland adenoma (*d* and *e*), papilloma (*f* and *g*), and squamous cell carcinoma (*h* and *i*) derived from K5.COX-2/667^{+/-} transgenics. [Magnification: *d*, *f*, and *h*, ×50; *e* and *i*, ×160; *g*, *Inset*, ×400.]

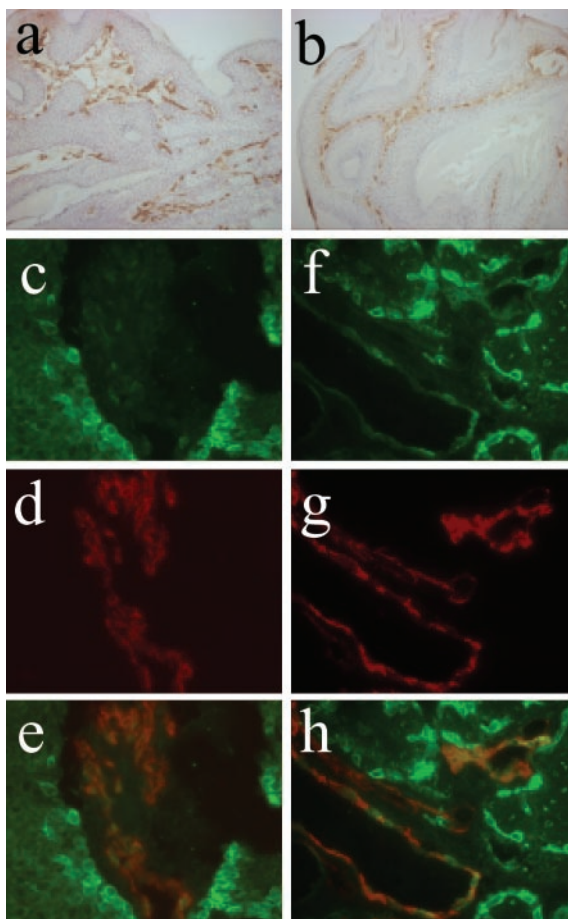


Fig. 5. Localization of COX-2 protein in the tumor vasculature. Tumor vasculature is visualized in a papilloma derived from a DMBA-initiated K5.COX-2/667^{+/-} transgenic mouse (a) and a DMBA/PMA-treated wt mouse (b) by immunostaining for the endothelial cell marker CD31. A double-immunofluorescence analysis was performed for a papilloma (c–e) and a sebaceous gland adenoma (f–h) from DMBA-initiated K5.COX-2/667^{+/-} transgenics by using anti-COX-2 and anti-CD31 antisera revealing that COX-2 (c and f, green) and CD31 (d and g, red) colocalize in tumor vessels (e and h, yellow). COX-2 expression is visible also in basal cells of papillomas and sebaceous gland adenomas (c and f). [Magnification: a and b, $\times 160$; c–h, $\times 630$.]

led to strongly increased epidermal levels of PGE₂, PGF_{2 α} , and 15-deoxy- $\Delta^{12,14}$ -PGJ₂ but not 6-keto-PGF_{1 α} (Fig. 4c).

Histological analysis of tumors identified sebaceous gland adenomas, papillomas, and squamous cell carcinoma (Fig. 4d–i). However, the relative frequency of the individual tumor types differed for DMBA-treated transgenics compared with DMBA/PMA-treated transgenics or wt mice. The ratio of papillomas plus squamous cell carcinomas to sebaceous gland adenomas was $\approx 1:1$ in DMBA-treated K5.COX-2/667^{+/-} mice but $\approx 4:1$ in DMBA/PMA-treated wt and transgenic mice. In addition, the ratio of carcinomas to papillomas was $\approx 1:5$ in DMBA-treated K5.COX-2/667^{+/-} as compared with $\approx 1:24$ and $1:35$ in DMBA/PMA-treated wt and K5.COX-2/667^{+/-} mice, respectively. Thus, in DMBA-treated K5.COX-2/667^{+/-} mice, both promotion and malignant progression of tumors were stimulated.

Tumor vascularization, as visualized by CD31 staining, was similar in papillomas derived from DMBA/PMA-treated wt and papillomas derived from K5.COX-2/667^{+/-} mice treated with DMBA alone (Fig. 5a and b). COX-2 expression in these tumors was found in the basal keratinocytes of papillomas (Fig. 5c; ref. 6) and basal cells of sebaceous gland adenomas (Fig. 5f). Moreover, double-immunofluorescence analysis for CD31 and

COX-2 revealed colocalization of the two proteins, i.e., indicating that COX-2 is expressed in the tumor vasculature (Fig. 5c–h). This effect was observed for tumors induced by initiation alone and by initiation/promotion.

Discussion

Tumor promotion is a critical event in cancer development and a potential target for chemopreventive measures. The multistage model of mouse skin carcinogenesis defines tumor development in terms of distinct stages and provides a standardized scheme for the investigation of tumor promoters. By using this model, a specific COX-2 inhibitor, celecoxib, was found to inhibit tumor formation by interfering with the promotion stage. Although COX-2 has been shown to catalyze the formation of genotoxic metabolites from polycyclic hydrocarbons (19), tumor initiation in skin by DMBA is not affected by celecoxib, whereas DMBA-induced breast cancer in rats was inhibited by this drug (7). Inhibition of postinitiation stages has also been observed for chemically induced colorectal carcinogenesis in rats (20). Thus, these studies indicate that COX-2 is involved in the promotion of both mouse skin and rat colon tumors.

As shown previously (15), transgenic overexpression of COX-2 in basal keratinocytes of mice results in a preneoplastic skin phenotype including epidermal hyperplasia and dysplasia and increased vascularization. Here we show that this phenotype depends on high levels of COX-2 expression and COX-2-mediated PG production as shown for line 667^{+/-} rather than the less pronounced COX-2 expression without concurrent PG production as in line 19^{+/-}. This result indicates that a distinct COX-2-expression level might be sufficient for the coupling with upstream phospholipases providing free arachidonic acid and downstream PG synthases converting PGH₂ to the final PG. Moreover, the development of the transgenic phenotype is suppressed in the presence of the COX-2-selective inhibitor valdecoxib, which prevents PG accumulation in the skin of transgenic mice. These results suggest a causal relationship between COX-2 expression, COX-2-mediated PG synthesis, and the development of the preneoplastic morphology. Spontaneous skin-tumor development, on the other hand, was an extremely rare event in these heterozygous transgenic mouse lines, indicating that COX-2 expression alone is not sufficient to induce skin-tumor formation.

The result of an initiation–promotion experiment with the K5.COX-2 transgenic mouse lines supports a cause-effect relationship for COX-2 overexpression and tumor development. In fact, skin-tumor development in high-expression transgenic mice requires initiation with DMBA, but a subsequent treatment with a tumor promoter is unnecessary. In contrast, wt animals and the low-expression transgenics develop tumors only after a combined initiator-promoter treatment. Thus, in NMRI mice, strong COX-2 overexpression and COX-2-mediated PG synthesis in basal keratinocytes generate an “autopromoted” skin phenotype, thereby mimicking the situation that occurs in wt skin after initiation and prolonged PMA treatment. The autopromoted state induced by overexpression of the COX-2 transgene dramatically increases the susceptibility of mouse skin for chemical carcinogenesis, which then only requires initiation by a “sub-threshold” DMBA treatment. On the other hand, treatment of the K5.COX-2 mice with DMBA plus PMA slightly decreased rather than increased the tumor response, indicating that constitutively increased levels of PG might interfere with PMA-induced tumor promotion as discussed previously for a K14.COX-2 mouse line (21, 22).

A strong mammary tumor response has been reported recently for mice with MMTV promoter-driven COX-2 overexpression (16). In this case multiparous but not virgin animals developed carcinomas at a high rate without any further treatment. However, a clear distinction between tumor initiation and tumor

promotion was not made, and thus the question of whether a discrete initiation event is required remains open.

The most frequent tumor type found in the skin of high-expression transgenics treated with DMBA alone were sebaceous gland adenomas that exhibited strong overexpression of COX-2 in basal sebocytes. In contrast, this tumor type was rare in wt and COX-2 transgenic mice treated with DMBA/PMA, indicating that the tumor promoter PMA not only causes COX-2 induction (6, 9) but also produces additional effects that evoke a cell type-specific tumor response. Interestingly, the levels of 15-deoxy $\Delta^{12,14}$ -PGJ₂ were increased strongly in the epidermis of high-expression transgenics compared with wt mice. Whether this PG, which is an activating ligand of the nuclear transcription factor peroxisome-proliferator-activated receptor γ (23), is involved in adenoma development remains to be clarified.

Another striking feature of the experiments presented here is the higher frequency of carcinoma formation for high-expression COX-2 transgenics treated with a single subthreshold DMBA dose alone compared with DMBA/PMA-treated wt or COX-2 transgenics, which suggests a stimulatory effect of COX-2 overexpression not only on promotion but also on malignant progression. Continuous PMA treatment, on the other hand, apparently favors papilloma formation but not malignant progression, in agreement with previous data that indicate that PMA decreases rather than increases malignant progression of papillomas (24).

The cellular events responsible for COX-2 effects on tumor development are not entirely clear at present. High levels of transgenic COX-2 delayed terminal differentiation of keratinocytes, leading to an expansion of the proliferative compartment of the epidermis (15). Intriguingly, COX-2 deficiency causes a premature terminal keratinocyte differentiation correlating with a reduced skin-tumor response after DMBA/PMA (13). Moreover, COX-2 overexpression may lead to a disturbance of cell-cell and cell-matrix interactions and the alteration of the epidermal architecture observed in transgenic epidermis (15),

also found for intestinal cells overexpressing COX-2 (25). In epidermis, these conditions may facilitate the selective growth and clonal expansion of initiated keratinocytes that carry a *ras* mutation caused by DMBA treatment (26). COX-2 overexpression, which induces basal cell hyperplasia, and *ras* mutation, which causes an additional defect in terminal differentiation of initiated cells (27), may synergistically support the clonal outgrowth of papillomas. Another protumorigenic effect of COX-2 seems to be the induction of neoangiogenesis required for nutritional support of tumors (28). Papillomas induced in DMBA-initiated high-expression transgenics exhibited no necrotic areas but a dense tumor vasculature similar to that of papillomas from DMBA/PMA-treated mice. A possible role for COX-2 in tumor angiogenesis has been suggested by other authors (29). COX-2-selective inhibitors impaired angiogenesis in rat cornea (30) and tumor xenografts (31). Moreover, COX-2 expression in the tumor-associated vasculature was observed also for tumor types other than epidermal (30). COX-2-derived PG from stromal endothelial and tumor cells may contribute to the angiogenic response.

If the model for mouse skin carcinogenesis is valid for other tissues and human carcinogenesis, then a strong, long-term COX-2 overexpression must be regarded as a substantial risk factor for cancer development. In view of the generally low concentrations of genotoxic carcinogens in the environment, our finding that COX-2 overexpression dramatically sensitizes a tissue for such agents may be of particular toxicological relevance.

We gratefully thank D. Kucher, S. Pfrang, B. Steinbauer, and A. Pohl-Arnold for excellent technical assistance, K. Seibert (Pharmacia, St. Louis) for kindly providing COX-2-selective inhibitors, Dr. A. Kopp-Schneider for statistical analysis, and Dr. W. Hull (both Deutsches Krebsforschungszentrum) for critical reading of the manuscript. This project was supported by a grant from the Deutsche Krebshilfe (eV, Bonn).

- Vane, J. R., Bakhle, Y. S. & Botting, R. M. (1998) *Annu. Rev. Pharmacol. Toxicol.* **38**, 97–120.
- Marks, F. & Fürstenberger, G. (2000) *Eur. J. Cancer* **36**, 314–329.
- Dannenberg, A. J., Altorki, N. K., Boyle, J. O., Dang, C., Howe, L. R., Weksler, B. B. & Subbaramaiah, K. (2001) *Lancet* **2**, 544–551.
- Gupta, R. A. & DuBois, R. N. (2001) *Nat. Rev. Cancer* **1**, 11–21.
- Cao, Y. & Prescott, S. M. (2002) *J. Cell. Physiol.* **190**, 279–286.
- Müller-Decker, K., Kopp-Schneider, A., Seibert, K., Marks, F. & Fürstenberger, G. (1998) *Mol. Carcinog.* **23**, 36–44.
- Harris, R. E., Alshafie, G. A., Abou-Issa, H. & Seibert, K. (2000) *Cancer Res.* **60**, 2101–2103.
- Steinbach, G., Lynch, P. M., Phillips, R. K., Wallace, M. H., Hawk, E., Gordon, G. B., Wakabayashi, N., Saunders, B., Shen, Y., Fujimura, T., et al. (2000) *N. Engl. J. Med.* **342**, 1946–1952.
- Müller-Decker, K., Scholz, K., Marks, F. & Fürstenberger, G. (1995) *Mol. Carcinog.* **12**, 31–41.
- Müller-Decker, K., Reinert, G., Krieg, P., Zimmermann, R., Heise, H., Bayerl, C., Marks, F. & Fürstenberger, G. (1999) *Int. J. Cancer* **82**, 648–656.
- Buckman, S. Y., Gresham, A., Hale, P., Hruza, P., Anast, J., Masferrer, J. & Pentland, A. P. (1998) *Carcinogenesis* **19**, 723–729.
- Fischer, S. M., Lo, H., Gordon, G. B., Seibert, K., Kelloff, G., Lubet, R. A. & Conti, C. J. (1999) *Mol. Carcinog.* **25**, 231–240.
- Tiano, H. F., Loftin, C. D., Akunda, J., Lee, C. D., Spalding, J., Sessoms, A., Dunson, D. B., Rogan, E. G., Morham, S. G., Smart, R. C. & Langenbach, R. (2002) *Cancer Res.* **62**, 3395–3401.
- Oshima, M., Dinchuk, J. E., Kargman, S. L., Oshima, H., Hancock, B., Kwong, E., Trazaskos, J. M., Evans, J. F. & Taketo, M. M. (1996) *Cell* **87**, 803–809.
- Neufang, G., Fürstenberger, G., Heidt, M., Marks, F. & Müller-Decker, K. (2001) *Proc. Natl. Acad. Sci. USA* **98**, 7629–7634.
- Liu, C. H., Chang, S. H., Narko, K., Trifan, O. C., Wu, M.-T., Smith, E., Haudenschild, C., Lane, T. F. & Hla, T. (2001) *J. Biol. Chem.* **276**, 18563–18569.
- Penning, T. D., Talley, J. J., Bertenshaw, S. R., Carter, J. S., Collins, P. W., Docter, S., Graneto, M. J., Lee, L. F., Malecha, J. W., Miyashiro, J. M., et al. (1997) *J. Med. Chem.* **40**, 1347–1365.
- Talley, J. J., Brown, D. L., Carter, J. S., Graneto, M. J., Koboldt, C. M., Masferrer, J. L., Perkins, W. E., Rogers, R. S., Shaffer, A. F., Zhang, Y. Y., et al. (2000) *J. Med. Chem.* **43**, 775–777.
- Wiese, F. W., Thompson, P. A. & Kadlubar, F. F. (2001) *Carcinogenesis* **21**, 5–10.
- Reddy, B. S., Hirose, A., Lubet, R., Steele, V., Kelloff, G., Paulson S., Seibert, K. & Rao, C. V. (2000) *Cancer Res.* **60**, 293–297.
- Bol, D. K., Rowley, R. B., Ho, C., Bilz, B., Dell, J., Swerdel, M., Kiguchi, K., Muga, S., Klein, R. & Fischer, S. M. (2002) *Cancer Res.* **62**, 2516–2521.
- Fischer, S. M. (2002) *J. Environ. Pathol. Toxicol. Oncol.* **21**, 183–191.
- Forman, B. M., Tontonoz, P., Chen, J., Brun, R. P., Spiegelman, B. M. & Evans, R. M. (1995) *Cell* **83**, 803–812.
- Hennings, H., Shores, R., Mitchell, P., Spangler, E. R. & Yuspa, S. H. (1983) *Nature (London)* **304**, 67–69.
- Tsujii, M. & DuBois, R. N. (1995) *Cell* **83**, 493–501.
- Quintanilla, M., Brown, K., Ramsden, M. & Balmain, A. (1986) *Nature (London)* **322**, 78–80.
- Dlugosz, A. A., Cheng, C., Williams E. K., Dharai, A. G., Denning, M. F. & Yuspa, S. H. (1994) *Cancer Res.* **54**, 6413–6420.
- Tsujii, M., Kawano, S., Tsujii, S., Sawaoka, H., Mori, M. & DuBois, R. N. (1998) *Cell* **93**, 705–716.
- Leahy, K. M., Koki, A. T. & Masferrer, J. L. (2000) *Curr. Med. Chem.* **7**, 1163–1170.
- Masferrer, J. L., Leahy, K. M., Koki, A. T., Zweifel, B. S., Settle, S. L., Woerner, B. M., Edwards, D. A., Flickinger, A. G., Moore, R. J. & Seibert, K. (2000) *Cancer Res.* **60**, 1306–1311.
- Leahy, K. M., Ornberg, R. L., Wang, A., Koki, A. T. & Masferrer, J. L. (2002) *Cancer Res.* **62**, 625–631.